Optical Simulation of Nanostructured Silicon Surfaces

Gagik Ayvazyan
National Polytechnic University of Armenia
Yerevan, Armenia
e-mail: gagik.ayvazyan@polytechnic.am

Karen Ayvazyan
National Polytechnic University of Armenia
Yerevan, Armenia
e-mail: agagarm@gmail.com

Harutyun Dashtoyan
National Polytechnic University of Armenia
Yerevan, Armenia
e-mail: dashtoyan.h@gmail.com

***Abstract*—The optical properties of nanostructured silicon surfaces in the form of nanocylinder and nanocone arrays are simulated by the finite difference time domain method. Such surfaces correspond to porous and black silicon layers, respectively. The relationship between the reflectance and the geometric parameters (in-plane period, out-of-plane depth or height, diameter) of the nanocylinders and nanocones has been studied. It is shown that surfaces with nanocones are the most effective frontal antireflective surfaces for solar cells.**

***Keywords*— Simulation, optical properties, porous silicon, black silicon.**

I. Introduction

Nanostructured silicon-based surfaces feature unique electronic and optical properties, high surface-to-volume ratios, and facile surface modification. Such sub-wavelength surfaces are a promising approach to reducing broadband light reflection for single junction and tandem silicon solar cells [1-3]. The first identified nanostructured silicon surface was the porous silicon (PS) layer, which can be considered as crystalline silicon with a nanovoid network [1]. In recent years, another nanostructured silicon surface, namely the black silicon (BS) layer, has been of greatest interest [2, 3]. This layer consists of an array of randomly arranged and densely packed nanoneedles. It is important to note that the PS and BS formation process is self-organized without additional external techniques.

Various properties of PS and BS depend on the geometrical parameters (diameter, period, height or depth) of nanopore and nanoneedle arrays [4-7]. Optical simulation of these surfaces can effectively optimize their parameters at the initial stage of solar cell design. Such an analysis eliminates the need for numerous experimental and technological reworks later. In addition, from the point of view of practical application, it is important to compare the antireflective properties of PS and BS with the same geometric parameters.

Various rigorous methods such as the finite difference time domain method (FDTD), the effective index technique, the rigorous coupled-wave analysis, the transfer matrix and finite element methods allow optical simulation of sub-wavelength surfaces [8-11]. The FDTD method is known for its accuracy and simplicity in modeling antireflective properties of nanostructured silicon-based surfaces.

In this work, using the FDTD method, we simulated and carried out a comparative analysis of the optical properties of PS and BS. Our research will improve the efficiency of solar cells with frontal antireflective surfaces based on self-organized nanopore and nanoneedle arrays.

II. Simulation Model Description

For simulation, we used the Rough Surface module of the commercial software package FDTD Solutions by Lumerical Co, which was previously used by us to simulate the optical properties of tandem structures with a BS interlayer [12]. This software package allows you to determine the optical properties of periodic structures depending on their shape and geometric dimensions, as well as on the wavelength and incidence angle of light radiation (θ) The numerical calculation is based on the parameters of stochastic nanostructured surfaces, namely, on the values of the root mean square (RMS), correlation length (LC) and spatial resolution (δ).

Based on the results of studying the PS and BS morphology [4, 5], their optical models can be represented as a thick silicon substrate with regular near-surface straight circular nanocylinders and nanocones, respectively (Fig.1, a). Such periodic structures can be characterized by the following basic parameters: in-plane period (t), out-of-plane depth or height (h) and diameter (d) (Fig.1, b). Based on these geometric parameters, the initial parameters RMS, δ, and LC required for simulation are uniquely determined (Fig.1, c).

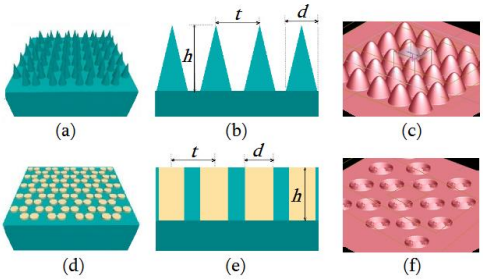

Fig. 1. Schematic diagrams of 3D view (a, d), cross-sectional view (b, e), and FDTD Solutions models (c, f) of simulated surfaces with nanocones (a, b, c) and nanocylinders (d, e, f)

https://doi.org/10.51408/csit2023_41

The simulation was carried out at normal ($\theta = 0^o$) and different angles of incidence of light radiation. The reference solar spectrum AM 1.5G was used to calculate the weighted average reflectance (WAR) of the simulated surfaces over $\lambda = 400 - 1000\,nm$ wavelength region according to the equation [12]

$$WAR(\lambda) = \frac{\int_{400nm}^{1000nm} R(\lambda)S(\lambda)_{AM1.5}d\lambda}{\int_{400nm}^{1000nm} S(\lambda)_{AM1.5}\,d\lambda},$$

where $R(\lambda)$ and $S(\lambda)_{AM1.5}$ are the wavelength-dependent reflection and incident photon flux of the AM1.5G solar spectrum, respectively.

III. Simulation Results

The reflectance, absorptance and transmittance spectra of simulated silicon surfaces with nanocylinders and nanocones for a wide range of wavelength at $\theta = 0^o$ are shown in Fig. 2. Surfaces with the following typical values of geometrical parameters were considered: h =650 nm, d =150 nm and t=250 nm. The optical properties of the plane silicon surface are used for comparison.

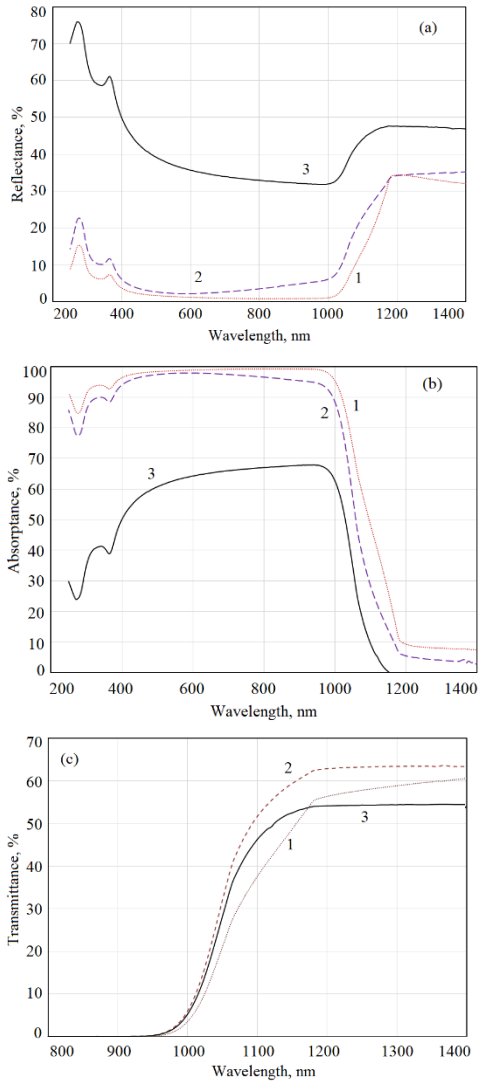

Fig. 2. Reflectance (a), absorptance (b) and transmittance (c) spectra of simulated surfaces with nanocylinders (1) and nanocones (2) and plane silicon surface (3)

It can be seen that the plane silicon surface is noticeably inferior to nanostructured surfaces in terms of optical properties. The most preferred are surfaces with nanocones, which correspond to BS.

Fig. 3 shows 2D WAR patterns of the simulated surfaces depending on the height and period of nanocylinders and nanocones at $\theta = 0^o$ and d=150 nm. The WAR values for different d at h=650 nm and t=250 nm are given in Table 1. It follows from the presented results that the reflectance strongly depends on the geometrical parameters of the nanostructured surfaces. WAR decreases as t decreases and h and d increase. This trend is more pronounced for surfaces with nanocones.

Table 1. The WAR values (%) for different diameters of nanocylinders and nanocones

Surface/Diameter	100 nm	150 nm	200 nm	250 nm
Nanocylinder	6.95	4.21	3.89	-
Nanocone	2.31	1.26	1.14	0.98

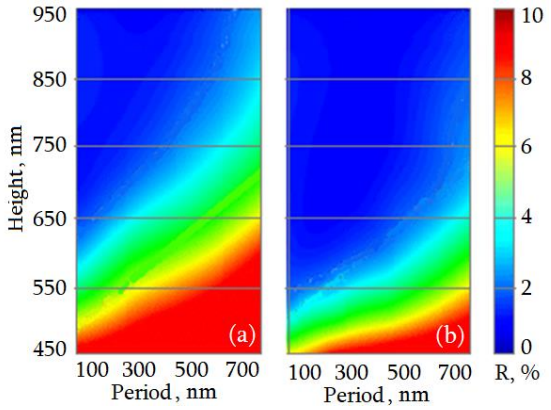

Fig. 3. 2D WAR patterns of the simulated surfaces with nanocylinders (a) and nanocones (b) depending on the height and period

2D reflectance patterns of the simulated surfaces at $\theta = 20 - 80^o$, normalized to the reflectance of the plane silicon surface, are shown in Fig. 4.

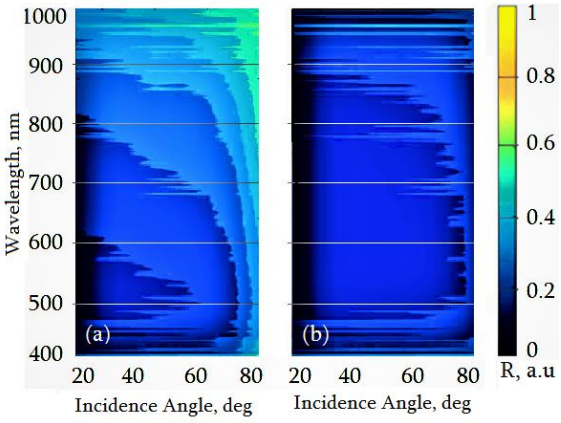

Fig. 4. 2D reflectance patterns of the simulated surfaces with nanocylinders (a) and nanocones (b), normalized to the reflectance of plane silicon surface

It can be seen that the nanostructured surfaces in the entire range of the incidence angle have a lower reflectance than plane silicon surfaces. The reflectance of surfaces with nanocones practically does not change at incidence angles less than 70°. In comparison with them, the reflectance of surfaces with nanocylinders noticeably increases starting from the incidence angle $\theta = 55^o$. The omnidirectional light trapping capability of the simulated surfaces is very important for photovoltaic stations without sun tracking to generate electricity in the morning and evening.

The results obtained indicate that, under all identical conditions, the simulated surfaces with nanocones are noticeably superior in antireflective properties to surfaces with nanocylinders. In the literature, the antireflective behavior of nanostructured silicon-based surfaces is associated with the combined action of the following two mechanisms [1, 3]: multiple reflections from neighboring textures and refractive index gradient change in the surface from air to silicon. From the point of view of the first mechanism, a better antireflective behavior of PS should be expected, since the area of light-receiving surfaces of nanocylinders is larger than that of nanocones. Therefore, it can be assumed that the second mechanism is predominant for the simulated surfaces. In this case, the refractive index gradient change is described by the following expression [13]:

$$n(z) = \left[f(z)n_{\mathrm{Si}}^{2/3} + 1 - f(z)\right]^{3/2},$$

where n_{Si} is the refractive index of silicon, $f(z)$ is the filling factor of the nanostructured surface, and the z axis is directed from the top to the base of the texture.

The refractive index gradient change of the simulated surfaces with nanocylinders and nanocones from air to silicon is schematically shown in Fig. 5. The boundary conditions for this change are as follows: $f(0) = 0,\ n(0) = n_{\mathrm{Air}} = 1$ and $f(h) = 1,\ n(h) = n_{\mathrm{Si}} = 3.8$. Unlike surfaces with nanocylinders, for which the refractive index change is abrupt, for surfaces with nanocones, the change occurs smoothly. It is well known that in this case, the antireflective behavior of the surfaces and films is more effective [11, 13]. Moreover, with an increase in f and h, the area of the light-receiving surface increases and the refractive index changes more smoothly, which together leads to a decrease in $R(\lambda)$ and WAR. This explains the observed dependencies of the simulated surfaces.

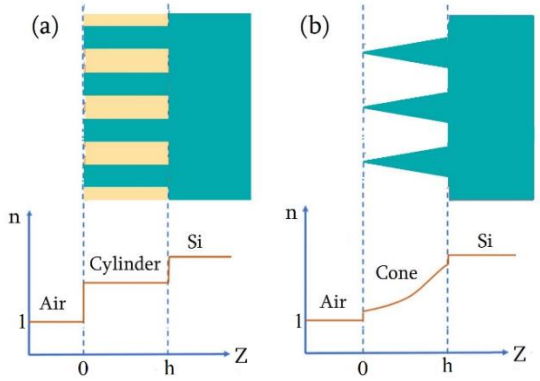

Fig. 5. Refractive index change of the simulated surfaces with nanocylinders (a) and nanocones (b)

Thus, the simulation results show that, from a practical point of view, it is expedient to use BS as a frontal antireflective surface of solar cells. This material has other advantages compared to PS, in particular, it is formed without the use of wet etchants, and the process is well-regulated and controlled. It is also important that the formation of BS does not depend on the crystallographic orientation of the initial silicon wafers.

IV. Conclusion

Porous and black silicon were presented as nanostructured surfaces with nanocylinders and nanocones to simulate the optical properties. Using the FDTD method, their reflectance, absorptance and transmittance spectra were determined. It is shown that the antireflective behavior of the simulated surfaces is mainly due to the refractive index gradient change. Surfaces with nanocylinders are noticeably inferior in antireflective properties to surfaces with nanocones, which indicates the promising use of black silicon in solar cells.

Acknowledgment

The study was carried out with the financial support of the Science Committee of the Republic of Armenia within the framework of Scientific Project No. 21AG-2B011.

References

[1] M. K. Sahoo and P. Kale, "Restructured Porous Silicon for Solar Photovoltaic: A Review", *Microporous & Mesoporous Mat.*, vol. 289, p. 109619, 2019.

[2] A. Vaseashta, G. Ayvazyan, S. Khudaverdyan and L. Matevosyan, "Structural and Optical Properties of Vacuum-Evaporated Mixed-Halide Perovskite Layers on Nanotextured Black Silicon", *Phys. Status Solidi RRL*, vol. 17, p. 2200482, 2023.

[3] M. Otto, M. Algasinger, H. Branz and B. Gesemann, "Black Silicon Photovoltaics", *Adv. Opt. Mat.*, vol. 3, no. 2, pp. 147--164, 2015.

[4] G. Ayvazyan, A. Vaseashta, F. Gasparyan and S. Khudaverdyan, "Effect of Thermal Annealing on the Structural and Optical Properties of Black Silicon", *J. Mater Sci: Mater. Electron.*, vol. 33, pp. 17001--17010, 2022.

[5] N. Selmane, A. Cheknane and H. S. Hilal, "Optimizing Optical and Electrical Properties of Porous Silicon by Enhancing Morphology through Substrate Type and Electro-Etching Control", *JOM*, vol. 75, pp. 1230--1241, 2023.

[6] G. Ayvazyan, L. Hakhoyan, K. Ayvazyan and A. Aghabekyan. "External Gettering of Metallic Impurities by Black Silicon Layer", *Phys. Status Solidi A*, vol. 220, no. 5, p. 220079, 2023.

[7] Y. A. Peschenyuk, A. A. Semenov and E. Y. Gatapova, "The Final Stage of Droplet Evaporation on Black Silicon by Schlieren Technique with a Graded Filter", *Experiments in Fluids*, vol 64, no. 1, pp. 1--10, 2023.

[8] K. Han and Chih-Hung Chang, "Numerical Modeling of Sub-Wavelength Anti-Reflective Structures for Solar Module Applications", *Nanomaterials*, vol. 4, pp. 87--128, 2014.

[9] G. Ayvazyan, F. Gasparyan and V. Gasparian, "Optical Simulation and Experimental Investigation of the Crystalline Silicon/Black Silicon/Perovskite Tandem Structures", *Optical Materials*, vol. 140, p. 113879, 2023.

[10] T. Rahman and S. Boden, "Optical Modelling of Black Silicon for Solar Cells using Effective Index Techniques", *IEEE J. of Photovolt.*, vol. 7, no. 6, pp. 1556--1562, 2017.

[11] M. Bellingeri, A. Chiasera, I. Kriegel and F. Scotognella, "Optical Properties of Periodic, Quasi-periodic, and Disordered One-dimensional Photonic Structures", *Optical Materials*, vol. 72, pp. 403--421, 2017.

[12] G. Y. Ayvazyan, D. L. Kovalenko, M. S. Lebedev, L. A. Matevosyan and A. V. Semchenko, "Investigation of the Structural and Optical Properties of Silicon-Perovskite Structures with a Black Silicon Layer" *J. of Contemporary Physics (Armenian Academy of Sciences)*, vol. 57, no 3, pp. 274--279, 2022.

[13] S Kim, G. S. Jeong, N. Y. Park and J.-Y. Choi, "Omnidirectional and Broadband Antireflection Effect with Tapered Silicon Nanostructures Fabricated with Low-Cost and Large-Area Capable Nanosphere Lithography", *Micromachines*, vol. 12, no. 2, pp. 119--206, 2021.